PROCEEDINGS OF SCIENCE

Testing the strength of the $\mathrm{U}_A(1)$ anomaly at the chiral phase transition in two-flavour QCD

Bastian B. Brandt[*], **Owe Philipsen**
Institute für Theoretische Physik, Goethe Universität, Max-von-Laue-Strasse 1, 60438 Frankfurt am Main, Germany
E-mail: brandt@th.physik.uni-frankfurt.de

Marco Cè
Helmholtz-Institut Mainz, Johannes Gutenberg-Universität Mainz, Germany

Anthony Francis
Theoretical Physics Department, CERN, CH-1211 Geneva 23, Switzerland

Tim Harris
Dip. di Fisica G. Occhialini, Università di Milano-Bicocca, and INFN, Sezione di Milano-Bicocca, Piazza della Scienza 3, I-20126 Milano, Italy

Harvey B. Meyer, Hartmut Wittig
PRISMA Cluster of Excellence and Institut für Kernphysik and Helmholtz-Institut Mainz, Johannes Gutenberg-Universität Mainz, Germany

We study the thermal transition of QCD with two degenerate light flavours by lattice simulations using $\mathcal{O}(a)$-improved Wilson quarks. Particular emphasis lies on the pattern of chiral symmetry restoration, which we probe via the static screening correlators. On lattices with a spatial extent of 32 lattice points we observe that the screening masses in transverse iso-vector vector and axial-vector channels become degenerate at the transition temperature. The splitting between the screening masses in iso-vector scalar and pseudoscalar channels is strongly reduced compared to the splitting at zero temperature and is actually consistent with zero within uncertainties. In this proceedings article we extend our studies to matrix elements and iso-singlet correlation functions. Furthermore, we present results on larger volumes, including first results at the physical pion mass.

The 9th International workshop on Chiral Dynamics
17-21 September 2018
Durham, NC, USA

[*]Speaker.

PoS(CD2018)055

1. Introduction

One of the peculiar features of Quantum Chromodynamics (QCD) is the spontaneous and explicit breaking of chiral symmetry. In the case with two massless quark flavours the theory is invariant under global transformations with elements of

$$\mathrm{SU}_L(2) \times \mathrm{SU}_R(2) \times \mathrm{U}_A(1) \times \mathrm{U}_V(1)\,. \tag{1.1}$$

The $\mathrm{U}_A(1)$ symmetry, however, is anomalously broken on the quantum level due to the Adler-Bell-Jackiw, or chiral, anomaly. In particular, the conservation equation for the axial vector current reads

$$\partial_\mu A^j_\mu(x) = -\delta_{j0}\frac{N_f\, g_0^2}{32\pi^2}\varepsilon^{\alpha\beta\mu\nu}\mathrm{Tr}\big[F_{\alpha\beta}(x)F_{\mu\nu}(x)\big] = -\delta_{j0}N_f Q(x)\,, \tag{1.2}$$

where $Q(x)$ denotes the operator associated with the topological charge density and

$$A^j_\mu(x) = \bar\psi(x)\gamma_\mu\gamma_5(\tau^j/2)\psi(x)\,, \tag{1.3}$$

is the axial current, including the Pauli matrices τ^j for $j = 1,2,3$ and $\tau^0 = \mathbf{1}$. Due to this anomalous breaking, the spontaneous breaking of chiral symmetry leads to three Goldstone bosons only, neutral and charged pions, while the η' meson retains a finite mass, even for vanishing light quark masses [1, 2].

The fate of the anomalous breaking of the $\mathrm{U}_A(1)$ symmetry at finite temperature plays a key role for the properties of the QCD phase diagram. In particular, the phase transition in the chiral limit of the light (u and d) quarks is sensitive to the possible restoration of the $\mathrm{U}_A(1)$ symmetry at the critical temperature, which could change the order and/or the universality class of the transition (see Refs. [3, 4, 5]). The two possible scenarios for the QCD phase diagram in dependence of the masses of the three lightest quarks are shown in Fig. 1. In scenario (1), the 2nd order chiral critical line reaches the $m_{ud} = 0$ axis in a tricritical point at m_s^{tric}, rendering the chiral transition 2nd order from this point on. The universality class in this scenario depends on the strength of the breaking of $\mathrm{U}_A(1)$ at the chiral transition. If the effect of the breaking is negligible, i.e. the symmetry effectively restored, the transition will be in the $\mathrm{U}(2)\times\mathrm{U}(2) \to \mathrm{U}(2)$ [4, 5] universality class (alternatively a $\mathrm{SU}(2)\times\mathrm{SU}(2)\times Z_4 \to \mathrm{SU}(2)$ universality class has also been proposed [6]) rather than in the standard $\mathrm{O}(4)$ universality class [3] for a substantial breaking of $\mathrm{U}_A(1)$. It is also possible that the restoration of the $\mathrm{U}_A(1)$ symmetry is sufficient to keep the transition first order for all values of the strange quark mass [3]. This is scenario (2) in Fig. 1. The question which of the two scenarios is realised is the only remaining completely open qualitative question of the phase diagram at vanishing chemical potential. Among the main problems to answer this questions are the inability to simulate directly in the chiral limit and the similarity of the different types of scaling behaviour. Investigating the fate of the $\mathrm{U}_A(1)$ symmetry at the chiral phase transition offers a viable alternative to the above methods (see our earlier paper [7] for a more detailed discussion and references).

The pattern of chiral symmetry restoration can be investigated using correlation functions of operators connected by the individual symmetries (see also [8]). One particular example are isovector correlation functions in vector $V^j_\mu(x) = \bar\psi(x)\gamma_\mu\gamma_5(\tau^j/2)\psi(x)$ and axial vector $A^j_\mu(x)$ channels, which are related by the $\mathrm{SU}_A(2)$ rotation. Consequently, the restoration of chiral symmetry

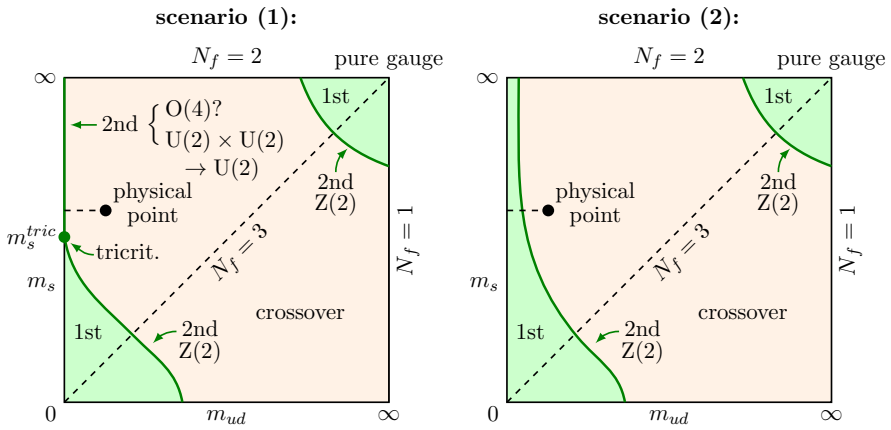

Figure 1: The two possible scenarios for the phase structure of QCD at zero chemical potential.

implies the degeneracy of the associated correlation functions. Of particular relevance for the $\mathrm{U}_A(1)$ symmetry are correlation functions in scalar and pseudoscalar channels. Including the iso-singlet operators (opening up new channels for the investigation of the effective symmetry restoration, see Ref. [9], for instance), they are related by $\mathrm{SU}_A(2)$ and $\mathrm{U}_A(1)$ transformations as shown in Fig. 2. The iso-vector operators P^i and S^i are comparably easy to compute on the lattice, due to the absence of disconnected diagrams, so that they have become the standard channels to look at to test for $\mathrm{U}_A(1)$ symmetry restoration. Since we are considering an effective restoration of the symmetry, we expect the renormalised correlation functions to become degenerate.

A number of studies have looked at the effective restoration of the $\mathrm{U}_A(1)$ symmetry in lattice QCD, mostly focussing on the low mode spectrum of the Dirac operator or chiral susceptibilities [10, 11, 12, 13, 14]. In contrast, we pursue a complementary approach, using the correlation functions, in particular, the screening masses. Screening masses probe the long distance properties of the correlation functions and are free of contact terms, which contaminate chiral susceptibilities, for instance. Apart from screening masses, the correlation functions include additional information in terms of matrix elements. The details of our strategy are explained in [7], where the iso-vector screening masses obtained from $N_t \times N_s^3 = 16 \times 32^3$ lattices have been published. N_t and N_s are temporal and spatial lattice extents in lattice units, respectively. Here we extend this study to larger volumes, the matrix elements of the correlation functions and present first results for iso-singlet screening masses, which provide additional information about the symmetry restoration pattern.

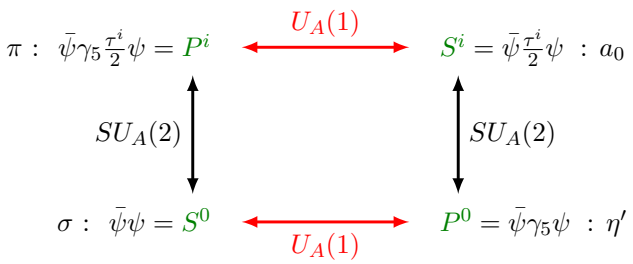

Figure 2: Transformation relations between iso-vector and iso-singlet operators in P and S channels.

scan	Volume	m_{ud} [MeV]	m_π [MeV]	T_c [MeV]	β_c	cfg
B1$_\kappa$	32^3	~ 41	~ 485	232(19)	5.465	~ 1000
C1	32^3	~ 17.5	300	211(6)	5.405	~ 400
C2	48^3					~ 1000
D1	32^3	~ 8.7	220	190(12)	5.340	~ 750
D2	48^3					~ 800
E2	48^3	~ 3.6	135	≈ 183	5.317	~ 400

Table 1: β-scans at $N_t = 16$. Listed are the lattice volume in lattice units, the quark mass m_{ud}, the zero-temperature pion mass m_π (estimated via NNLO χPT, see [7]), the critical temperature T_c, the critical lattice coupling β_c and the approximate number of independent configurations per ensemble 'cfg' (estimated via the integrated autocorrelation time of the plaquette at T_c). Scan **B1**$_\kappa$ has been done with a constant hopping parameter κ rather than at constant m_{ud}. The quoted quark and pion masses correspond to the ones at T_c. Note, that a spatial extent of $N_s = 16$ corresponds to a physical extent of about 1 fm at T_c. For scan **E2** the critical temperature has been estimated from the $\mathrm{O}(4)$ scaling fit to the $N_s = 32$ lattices [7].

Earlier accounts of our study have been reported in [15, 16, 17, 18].

2. Simulation Setup

We perform simulations with two flavours of $O(a)$ improved Wilson fermions [19], with the non-perturbatively estimated clover coefficient from Ref. [20], and Wilson's gauge action. The simulations employ deflation accelerated versions of the Schwarz [21, 22] and (twisted) mass [23, 24, 25] preconditioned algorithms. We vary the temperature by changing the lattice spacing via the lattice coupling β, keeping the temporal extent fixed at $N_t = 16$. For more details concerning the simulation algorithms, lines of constant physics and scale setting see [7]. In the approach to the chiral limit we use several quark masses and volumes to control finite size effects. A list of temperature scans with the results for the critical temperatures is given in Tab. 1

Our main observables are correlation functions in spatial direction, so called screening correlators [26]. For a particular mesonic operator O the screening correlation function is given by

$$C_O(x_\mu) = \int d^3x_\perp \left\langle O(x_\mu, \vec{x}_\perp) O^\dagger(0) \right\rangle . \tag{2.1}$$

Here x_μ (we take $x_\mu = z$) is the coordinate of the direction in which the correlation function is evaluated and $\vec{x}_\perp$ is the coordinate vector in the orthogonal directions. The equality of the renormalised correlation functions of channels related by a particular symmetry signals its effective restoration. Previously we have focussed on correlation functions with iso-vector operators, i.e. operators including a Pauli matrix τ^i, for which only quark connected correlation functions contribute. Here we will also present first results for quark disconnected correlation functions, enabling us to compute correlation functions in iso-singlet channels. The details will be discussed in Sec. 4.

On a periodic lattice of extent L_z, the leading order of the spectral representation, including only the groundstate contribution, of a correlation function $C_O(z)$ is given by

$$C_O(z) = \frac{|Z_O|^2}{M_O} \left(e^{-M_O z} + e^{-M_O (L_z - z)} \right) . \tag{2.2}$$

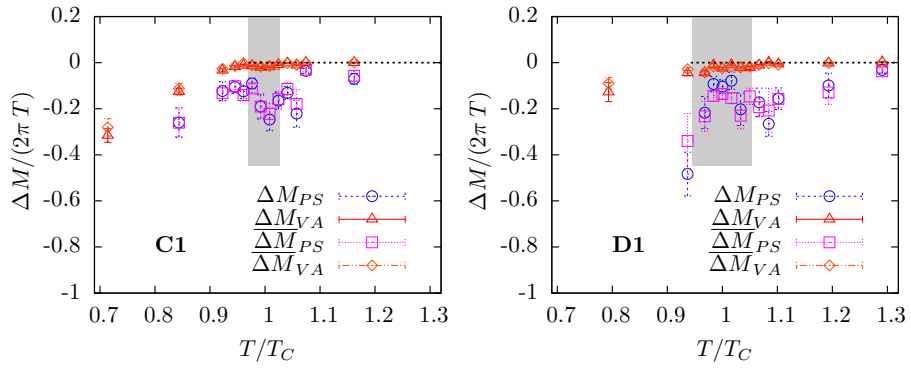

Figure 3: Results for the differences ΔM_{PS} and ΔM_{VA}, for scans **C1** (left) and **D1** (right). The differences are normalised to $2\pi T$. The grey area marks the transition region. The results indicated by $\overline{\Delta M}$ are an alternative estimate for the screening mass difference (see [7]).

The exponential decay of $C_O(x_\mu)$ with x_μ defines the 'screening mass' M_O in this channel and the proportionality constant contains the matrix element Z_O. Consequently, the equality of the correlation functions not only implies the equivalence of the screening masses, but also of the renormalised matrix elements $\mathscr{Z}_O Z_O$, where $\mathscr{Z}_O$ are the multiplicative renormalisation factors.

3. Anomalous Breaking of $\mathrm{U}_A(1)$ from Iso-Vector Correlation Functions

We start with the discussion of the results for correlation functions in the iso-vector channels. In particular, we look at the correlation functions from Eq. (2.1) in pseudoscalar P^i, scalar S^i, vector V^i and axial vector A^i channels. In this section we conveniently drop the superscript i for brevity. Iso-vector correlation functions include a connected part only, which we evaluate using point sources. We typically use 48 point sources per configuration with random starting positions. We first focus on the screening mass differences,

$$\Delta M_{O_1 O_2} = M_{O_1} - M_{O_2}\,, \tag{3.1}$$

which are direct measures for the effective restoration of the symmetries. These differences are extracted from plateaus in the effective masses of the ratios of the correlation functions in the individual channels, taking into account the leading order contributions from excited states.

The results for the screening mass differences on scans **C1** and **D1**, as obtained in [7], are shown in Fig. 3. We observe an approximate degeneracy of M_V and M_A, indicating the effective restoration of $\mathrm{SU}_A(2)$ at T_c. The difference ΔM_{PS} is non-vanishing at T_c, meaning $\mathrm{U}_A(1)$ is still broken for these quark masses. This finding is in qualitative and quantitative agreement with findings from staggered [27], domain wall [10, 28, 29] and overlap [11, 30] fermion formulations. In the approach to the chiral limit the difference decreases. To obtain an estimate in the chiral limit we perform a linear chiral extrapolation of ΔM_{PS} (averaging over the transition region and using the spread of results as a systematic uncertainty; see Ref. [7]). The results from the averaging procedure for scans $\mathbf{B1}_\kappa$, **C1** and **D1** versus the quark mass are shown as the grey points in Fig. 5 together with their chiral extrapolation, the grey point at $m_{ud} = 0$. To enable an assessment whether the breaking is weak or strong in the chiral limit, Fig. 5 also includes a phenomenological estimate

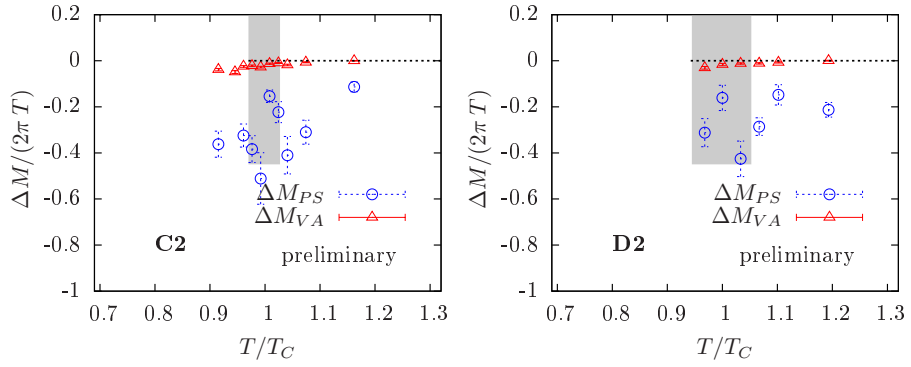

Figure 4: Results for the differences ΔM_{PS} and ΔM_{VA}, for scans **C2** (left) and **D2** (right).

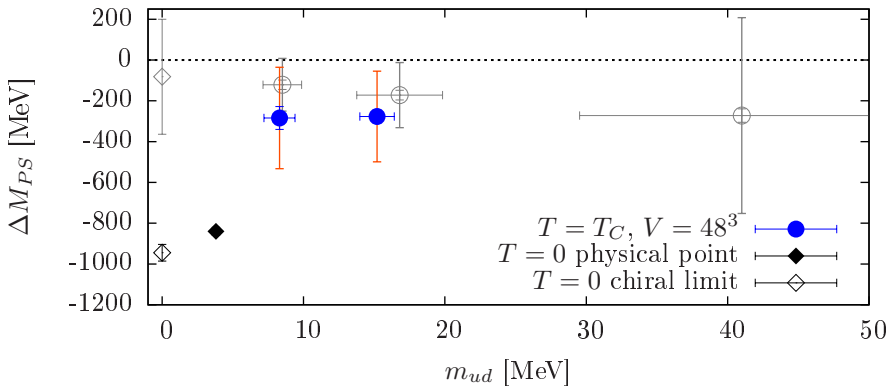

Figure 5: Results for ΔM_{PS} from the temperature scans with a volume of $N_s^3 = 48^3$. The grey points are the results from the $N_s^3 = 32^3$ volumes for comparison and the black points are the reference values at $T = 0$ (see text).

for the mass difference in the chiral limit and at the physical point in full QCD at $T = 0$ [7]. A comparison between the chiral extrapolation and the phenomenological estimate shows that the $\mathrm{U}_A(1)$ breaking screening-mass difference is comparably small at T_c, indicating a weak breaking or even a restoration of the $\mathrm{U}_A(1)$ symmetry at $m_{ud} = 0$.

For the $N_s^3 = (L/a)^3 = 32^3$ volumes and smaller quark masses, the value for $m_\pi L$, with m_π the $T = 0$ pion mass, becomes smaller than 3. To be able to extend the study to smaller quark masses and to test for finite size effects, we have thus repeated the computations on $N_s^3 = 48^3$ lattices. The results for the screening mass differences on these new scans **C2** and **D2** are shown in Fig. 4. While the results for ΔM_{VA} look very similar to the ones from scans **C1** and **D1**, ΔM_{PS} tends to become larger with increasing volume. The result for ΔM_{PS} at T_c, once more averaged over the transition region, are shown in Fig. 5. One can see the tendency towards larger screening mass differences with increasing volume. This tendency seems to remain for the chiral limit. To perform a reliable chiral extrapolation, however, we need to extend the simulations to smaller quark masses and increase the statistics for scan **D2**.

To extend our study to smaller quark masses we have started a temperature scan at the phys-

ical pion mass, labelled **E2** in Tab. 1. So far only results at $T > T_c$ (T_c estimated using O(4) scaling [7]) are available, for which we have performed measurements with 16 point sources per configuration. The results are shown in Fig. 6. While the results for $T/T_c > 1.1$ indicate a smaller value for ΔM_{PS} the one at $T/T_c \approx 1.05$ is further away from zero as for scans **C2** and **D2** at similar values for T/T_c. The latter, however, lacks statistics and thus can still change considerably. We are currently increasing precision and are extending the runs to T_c and below.

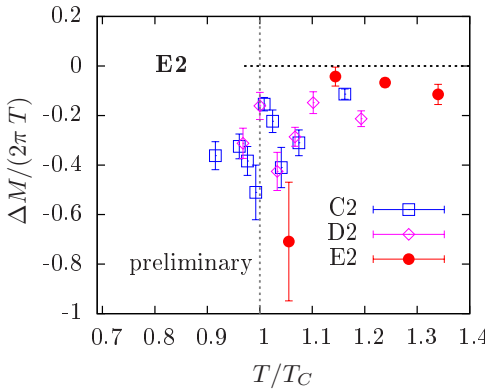

Figure 6: Results for the differences ΔM_{PS}, for scans **C2**, **D2** and **E2**.

An alternative observable extracted from correlation functions are the matrix elements Z_O from Eq. (2.2). In contrast to the screening masses, however, these observables demand multiplicative renormalisation. The analogue to ΔM_{PS} for the matrix elements is the renormalised difference

$$\Delta Z_{PS} = \mathscr{Z}_P |Z_P| - \mathscr{Z}_S |Z_S| \,. \tag{3.2}$$

For the determination of $\mathscr{Z}_P$, we have interpolated the results from [31] as discussed in [7]. The determination of $\mathscr{Z}_S$ is a bit more involved and we refer to the renormalisation of the chiral condensate in [7] for the details. The renormalised difference is plotted for scans **C1** and **D1** in Fig. 7. As the screening mass difference, ΔZ_{PS} remains non-zero at T_c. In contrast to ΔM_{PS}, however, ΔZ_{PS} shows a tendency to increase when the quark mass is lowered.

4. Iso-Singlet Screening Correlators

Iso-singlet correlation functions open up new channels to investigate the chiral symmetry restoration pattern. In two-flavour QCD with degenerate quark masses, the difference between iso-vector and iso-singlet correlation function is the presence of quark disconnected diagrams for the latter. In this section we will distinguish explicitly between iso-vector O^i and iso-singlet O^0 operators/correlation functions. Introducing quark connected $C^{\mathrm{conn}}_{\mathscr{O}}(z)$ and quark disconnected $C^{\mathrm{disc}}_{\mathscr{O}}(z)$

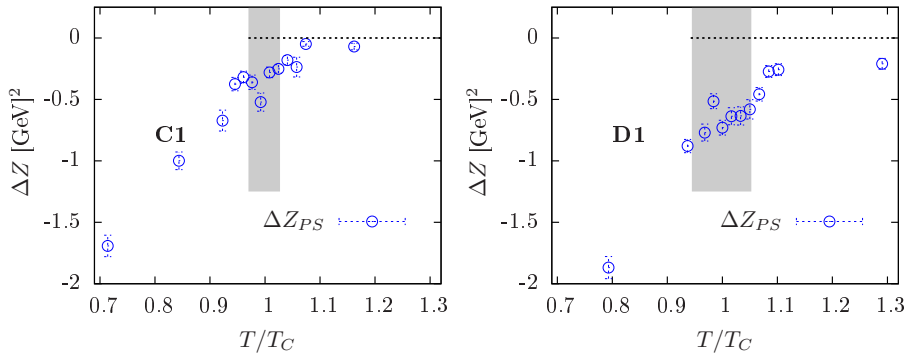

Figure 7: Results for the differences ΔZ_{PS}, for scans **C2** and **D2**.

correlation functions, defined by traces over quark propagators as depicted in Fig. 8, iso-vector and iso-singlet correlation functions of an operator O are given by,

$$C_{O^i}(z) = -\frac{1}{2}C^{\text{conn}}_{\mathscr{O}}(z) \quad \text{and} \quad C_{O^0}(z) = -\frac{1}{2}C^{\text{conn}}_{\mathscr{O}}(z) + C^{\text{disc}}_{\mathscr{O}}(z)\,. \tag{4.1}$$

Here $\mathscr{O}$ refers to the operator in Dirac and colour space only, excluding the flavour matrices from the operator O, and the correlation functions include only a single fermion propagator (since u and d propagators are indistinguishable in QCD when quark masses are degenerate). Note, that the iso-singlet correlation function might include a constant contribution, which is a finite size effect resulting from imperfect sampling of topological sectors [32]. The constant piece is absent in the shifted correlator $\tilde{C}(z) = C(z) - C(z+1)$ [33], which we use to fit the correlation function in the P^0 channel.

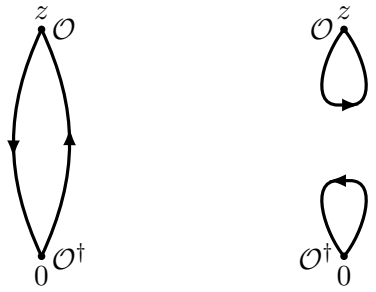

Figure 8: Graphical representation of quark connected (left) and disconnected (right) diagrams in lattice QCD.

We will focus on correlation functions in P and S channels at T_c. The transformation relations between iso-vector and iso-singlet channels are shown in Fig. 2. We see that the inclusion of the disconnected diagrams enables to test the effective restoration of both symmetries using P and S correlation functions. In particular, in the case that $\mathrm{SU}_A(2)$ is restored, for which we have seen indications above, we expect a degeneracy of P^0 and S^i, as well as P^i and S^0 correlation functions. If, the $\mathrm{U}_A(1)$ symmetry remains broken, correlation functions in P^i and S^i channels and P^0 and S^0 channels remain non-degenerate.

We will first compare the connected and disconnected parts of the correlation functions, shown in the left panel of Fig. 9. The disconnected correlation functions have been computed with 32 Hadamard probing vectors for hierarchical probing [34]. While the magnitude of connected and disconnected correlation functions in the P channel is similar, the disconnected correlator is negative, leading to a large cancellation. At $T = 0$ this cancellation results in the exponential decay of the iso-singlet correlator with the η' mass. In the S channel, both correlation functions are positive,

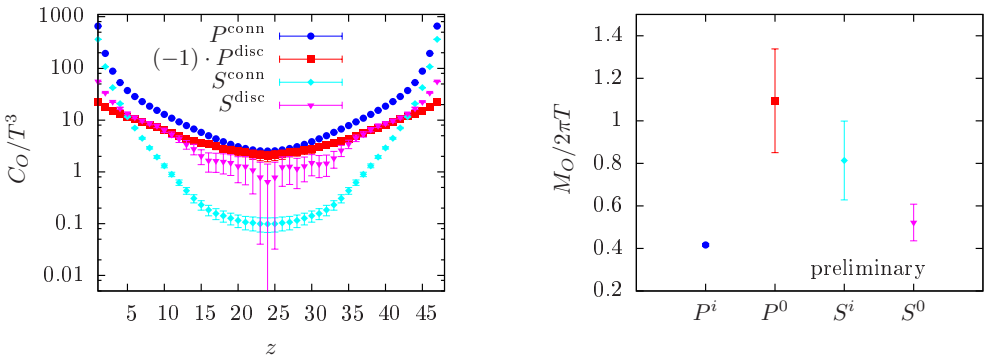

Figure 9: Screening correlation functions (left) and masses (right) for the different channels at the critical temperature of scan **C2**.

but the disconnected correlation function has a slower exponential decay and thus governs the iso-singlet correlator. To investigate the pattern of chiral symmetry restoration, we have extracted the iso-singlet screening masses from the correlators, which we compare to the iso-vector screening masses in the right panel of Fig. 9. Both, the screening masses in P^i and S^0 channels, as well as in P^0 and S^i channels agree within (their large) uncertainties, confirming the effective restoration of $\mathrm{SU}_A(2)$. At the same time, also the screening masses in P^0 and S^0 channels are non-degenerate, indicating a residual breaking of $\mathrm{U}_A(1)$, as seen in the previous section.

Note, that the results are preliminary in the sense that currently the statistics is not sufficient to extract the iso-singlet screening masses reliably. In particular, the screening masses in Fig. 9 (except for M_{P^i}) have been extracted without taking excited states into account. This is problematic since the signals become lost in noise already at comparably small values of z. The obvious next task is to increase statistics and to confirm the results presented in this section.

5. Conclusions

In this proceedings article we have updated our initial study [7] to larger volumes, showed first results for a scan at physical light quark masses, extended our set of observables and presented first results for the extension to iso-singlet correlation functions. Larger volumes show the tendency to strengthen the effect of the anomalous breaking of the $\mathrm{U}_A(1)$ symmetry. However, a chiral extrapolation of the screening mass difference at T_c is currently not possible for the larger volumes, lacking a third quark mass. We are currently extending our simulations to the physical quark mass, for which we have shown first results. Additional observables are renormalised matrix elements of the screening correlators. Evaluated on the $N_s^3 = 32^3$ volumes, they tend to show an increase in the strength of the breaking of $\mathrm{U}_A(1)$ for smaller quark masses. A first look at screening masses in iso-singlet channels at T_c for scan **C2** shows that the breaking of $\mathrm{U}_A(1)$ is also present in P^0 and S^0 channels, while invariance under $\mathrm{SU}_A(2)$ transformations appears to be restored. To be able to reliably extract information from the iso-singlet correlators, however, a substantial increase in precision is mandatory.

Acknowledgements:
B.B. would like to thank J. Ruiz de Elvira and Y. Aoki for stimulating discussions and the conveners of the GB Dynamics session for the invitation to present the results. We acknowledge computer time for the generation of the gauge configurations on the JUROPA, JURECA and JUQUEEN computers of the Gauss Centre for Supercomputing at FZ Jülich, allocated through the John von Neumann Institute for Computing (NIC) within project HMZ21. Parts of the simulations have been done on "Wilson" at the Institute for Nuclear Physics, University of Mainz, "Clover" at the Helmholtz-Institut Mainz and the FUCHS cluster at the Centre for Scientific Computing, University of Frankfurt. This work has been supported by the Cluster of Excellence PRISMA+ (EXC 2118/1), funded by DFG within the German Excellence Strategy (Project ID 39083149), the *Center for Computational Sciences in Mainz* as part of the Rhineland-Palatine Research Initiative and by DFG grant ME 3622/2-2 *QCD at finite temperature with Wilson fermions on fine lattices*. B.B. has also received funding by the DFG via SFB/TRR 55 and the Emmy Noether Programme EN 1064/2-1.

References

[1] E. Witten, Nucl. Phys. B **156** (1979) 269.

[2] G. Veneziano, Nucl. Phys. B **159** (1979) 213.

[3] R. D. Pisarski and F. Wilczek, Phys. Rev. D **29** (1984) 338.

[4] A. Butti, A. Pelissetto and E. Vicari, JHEP **0308** (2003) 029 [hep-ph/0307036].

[5] A. Pelissetto and E. Vicari, Phys. Rev. D **88** (2013) no.10, 105018 [arXiv:1309.5446].

[6] S. Aoki [JLQCD Collaboration], PoS CD **15** (2016) 045 [arXiv:1603.00997].

[7] B. B. Brandt *et al*, JHEP **1612** (2016) 158 [arXiv:1608.06882].

[8] A. Gomez Nicola and J. Ruiz de Elvira, Phys. Rev. D **97** (2018) no.7, 074016 [arXiv:1704.05036].

[9] A. Gomez Nicola and J. Ruiz De Elvira, Phys. Rev. D **98** (2018) no.1, 014020 [arXiv:1803.08517].

[10] A. Bazavov *et al.* [HotQCD Collaboration], Phys. Rev. D **86** (2012) 094503 [arXiv:1205.3535].

[11] G. Cossu *et al*, Phys. Rev. D **87** (2013) no.11, 114514 [arXiv:1304.6145].

[12] T. W. Chiu *et al.* [TWQCD Collaboration], PoS LATTICE **2013** (2014) 165 [arXiv:1311.6220].

[13] V. Dick *et al*, Phys. Rev. D **91** (2015) no.9, 094504 [arXiv:1502.06190].

[14] A. Tomiya *et al*, Phys. Rev. D **96** (2017) no.3, 034509 [arXiv:1612.01908].

[15] B. B. Brandt *et al*, PoS LATTICE **2010** (2010) 172 [arXiv:1008.2143].

[16] B. B. Brandt *et al*, AIP Conf. Proc. **1343** (2011) 516 [arXiv:1011.6172].

[17] B. B. Brandt *et al*, PoS LATTICE **2012** (2012) 073 [arXiv:1210.6972].

[18] B. B. Brandt *et al*, PoS LATTICE **2013** (2014) 162 [arXiv:1310.8326].

[19] B. Sheikholeslami and R. Wohlert, Nucl. Phys. B **259** (1985) 572.

[20] K. Jansen *et al.* [ALPHA Collaboration], Nucl. Phys. B **530** (1998) 185 [hep-lat/9803017].

[21] M. Lüscher, Comput. Phys. Commun. **165** (2005) 199 [hep-lat/0409106].

[22] M. Lüscher, JHEP **0712** (2007) 011 [arXiv:0710.5417].

[23] M. Hasenbusch, Phys. Lett. B **519** (2001) 177 [hep-lat/0107019].

[24] M. Marinkovic and S. Schaefer, PoS LATTICE **2010** (2010) 031 [arXiv:1011.0911].

[25] M. Lüscher and S. Schaefer, Comput. Phys. Commun. **184** (2013) 519 [arXiv:1206.2809].

[26] C. E. Detar and J. B. Kogut, Phys. Rev. Lett. **59** (1987) 399.

[27] M. Cheng *et al.*, Eur. Phys. J. C **71** (2011) 1564 [arXiv:1010.1216].

[28] T. Bhattacharya *et al.*, Phys. Rev. Lett. **113** (2014) no.8, 082001 [arXiv:1402.5175].

[29] G. Cossu *et al.* [JLQCD Collaboration], PoS LATTICE **2014** (2015) 210 [arXiv:1412.5703].

[30] A. Tomiya *et al*, PoS LATTICE **2014** (2015) 211 [arXiv:1412.7306].

[31] P. Fritzsch *et al*, Nucl. Phys. B **865** (2012) 397 [arXiv:1205.5380].

[32] S. Aoki *et al*, Phys. Rev. D **76** (2007) 054508 [arXiv:0707.0396].

[33] K. Ottnad *et al.* [ETM Collaboration], Phys. Rev. D **97** (2018) no.5, 054508 [arXiv:1710.07986].

[34] A. Stathopoulos *et al*, SIAM J. Sci. Comput. 35 (2013), 299 [arXiv:1302.4018].